Supporting Information
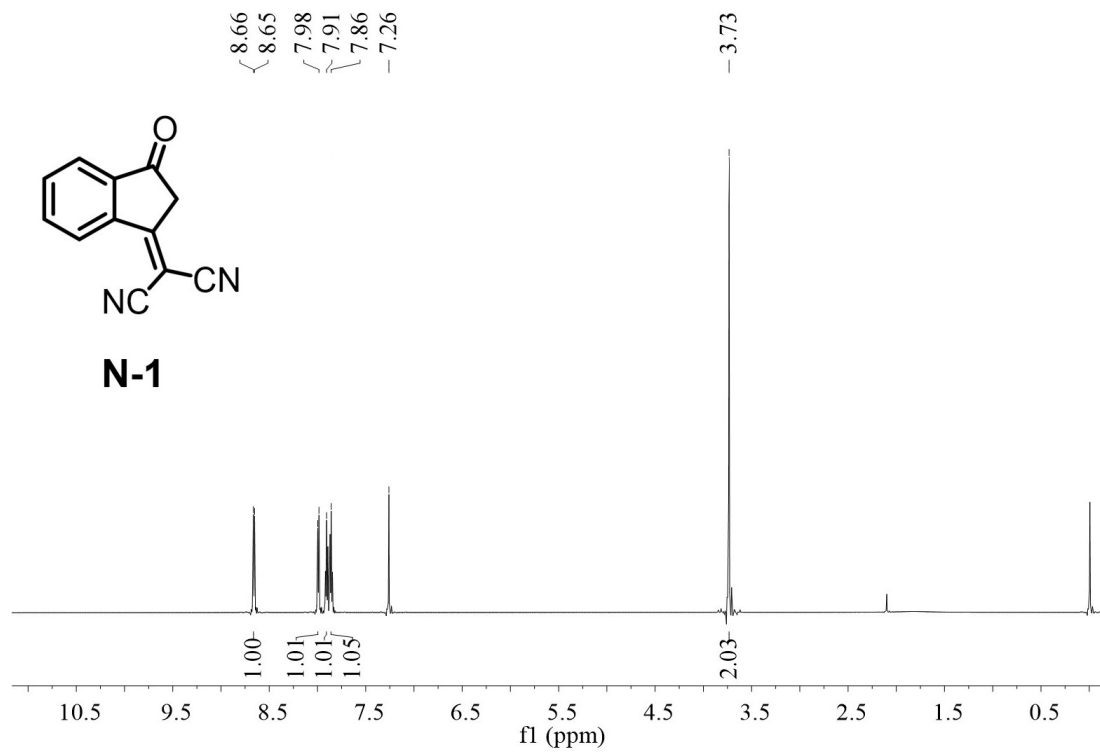
Injectable Thermosensitive Hydrogel to Enhance Photothermal Ablation and Systemic Immunotherapy of Breast Tumors

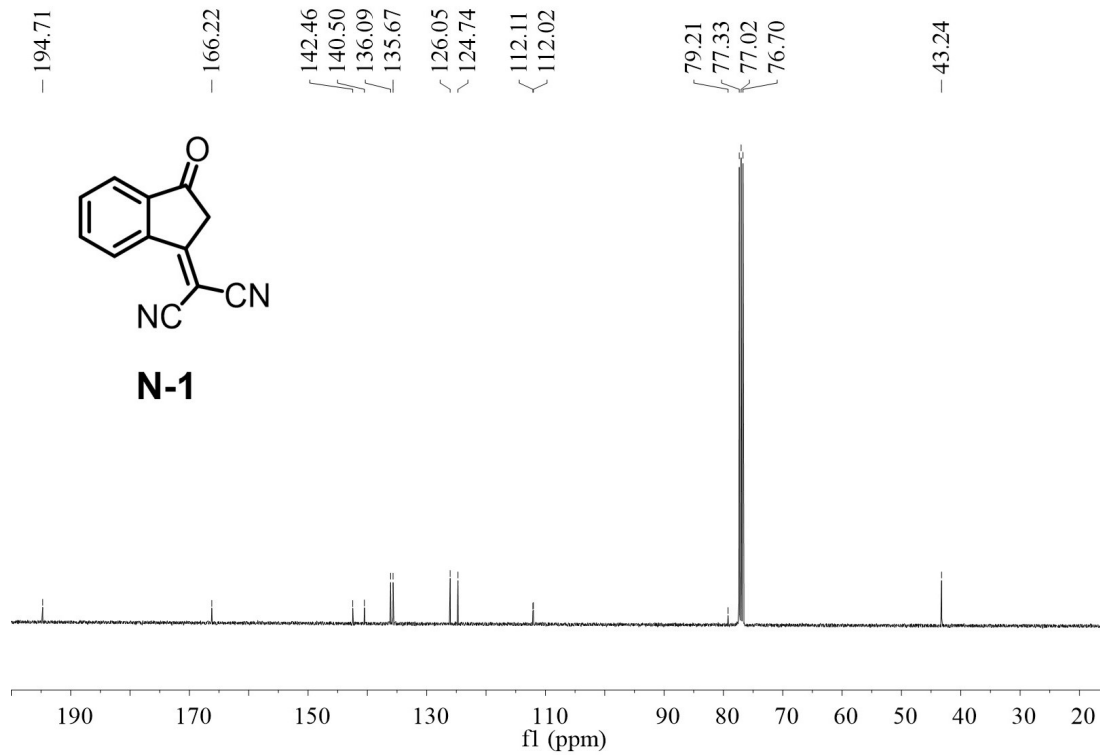*Tao Qin, Ruipeng Li, Huiqin Jin, Yunxia Wang* and Liheng Feng **

School of Chemistry and Chemical Engineering, Shanxi University, Taiyuan, 030006, P.R. China
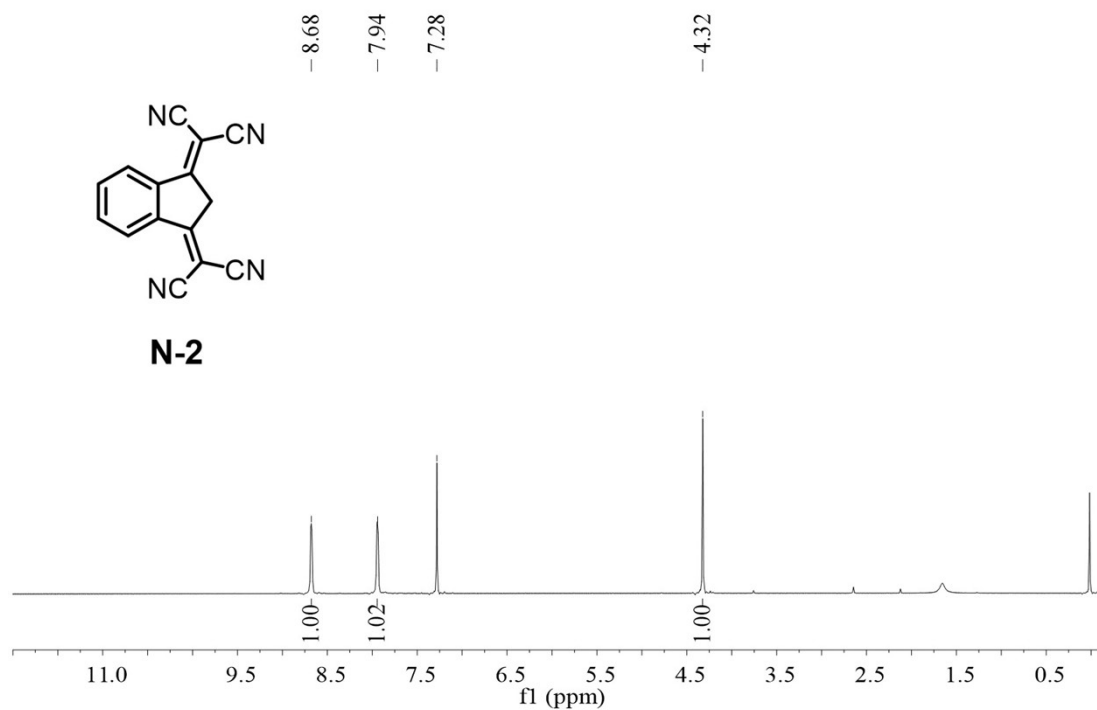
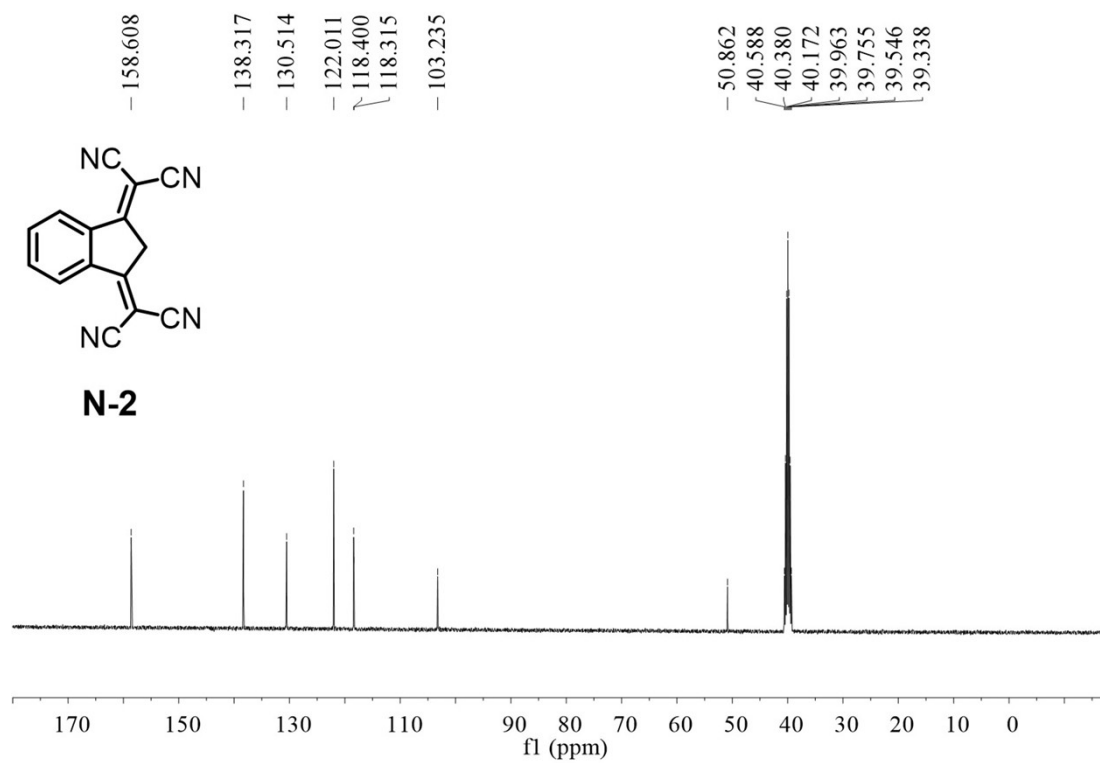E-mail: wangyunxia@sxu.edu.cn (Wang, Y.X.); lhfeng@sxu.edu.cn (Feng, L.H.)

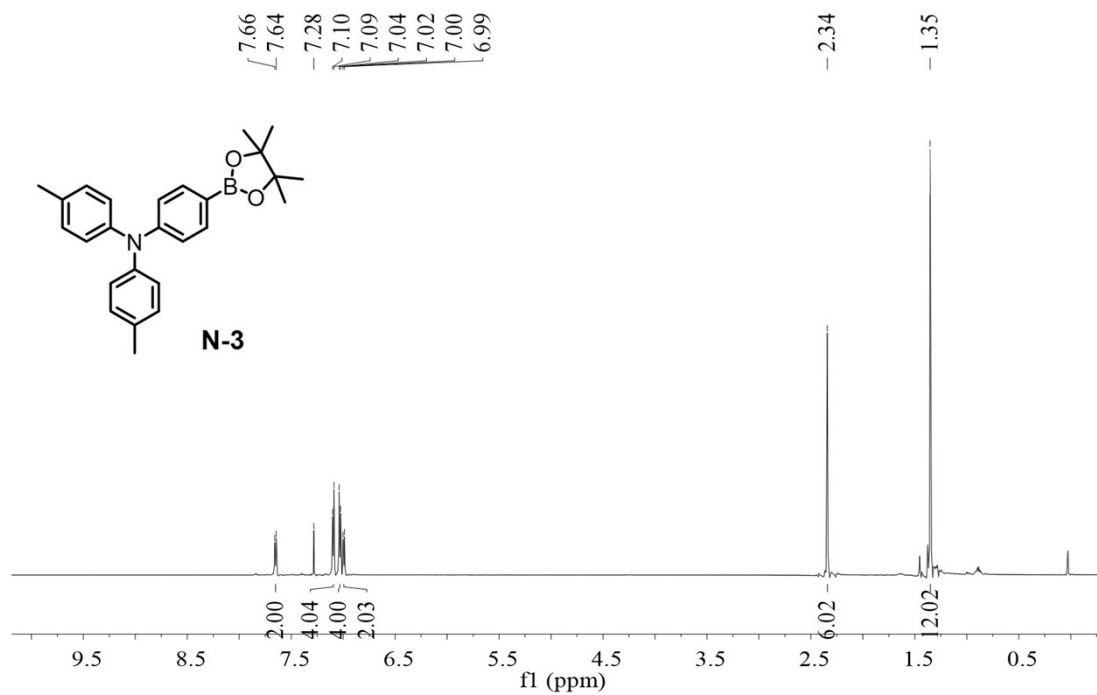*Fig. S1*. ^{1}H NMR spectrum of N-1 in CDCl$_3$.

Fig. S2. ^{13}C NMR spectrum of N-1 in CDCl$_3$.

Fig. S3. ^{1}H NMR spectrum of N-2 in CDCl$_3$.

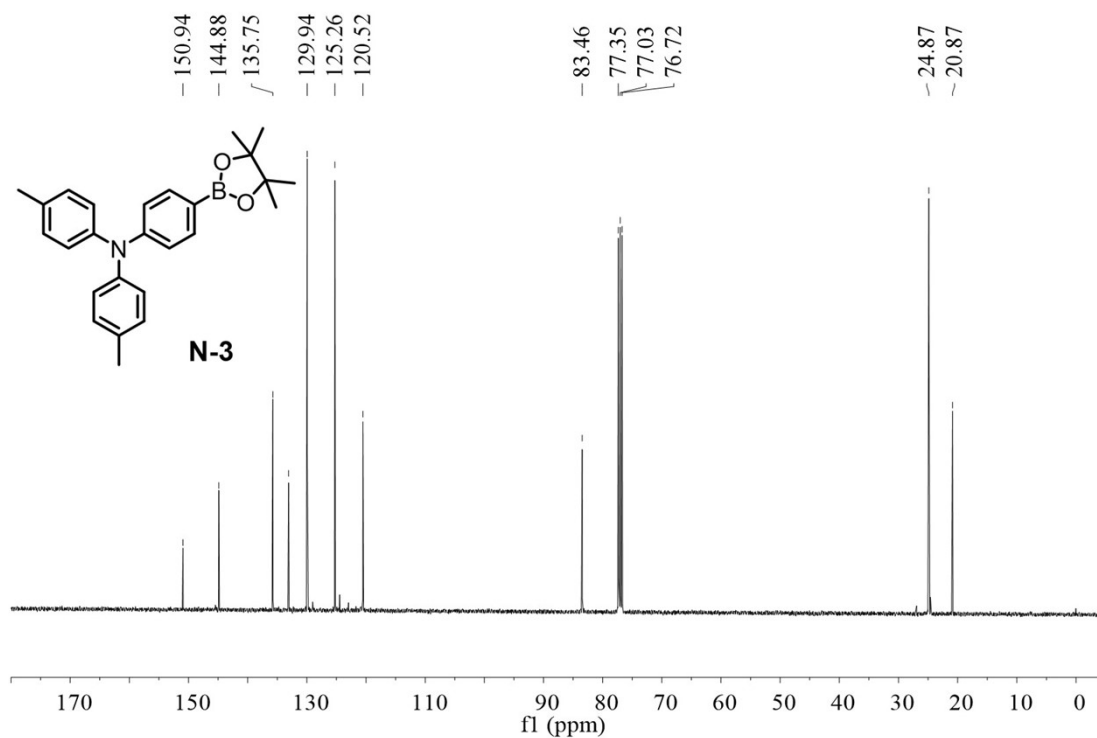**Fig. S4.** ^{13}C NMR spectrum of N-2 in DMSO-d_6.
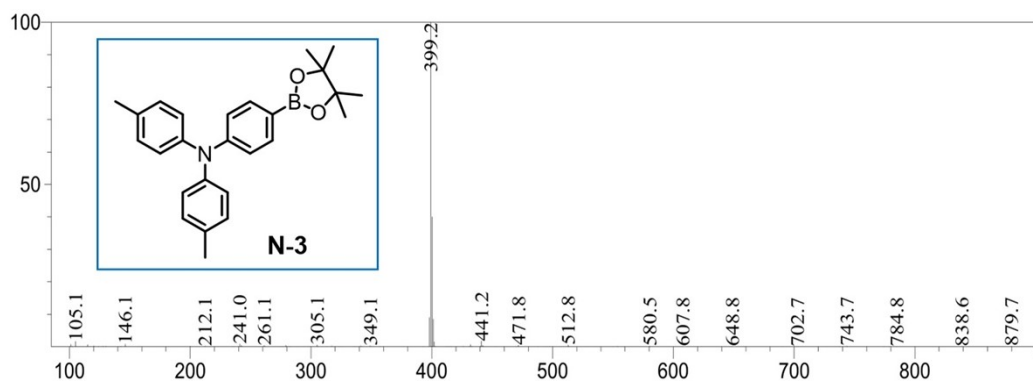
Fig. S5. LCMS of N-3.

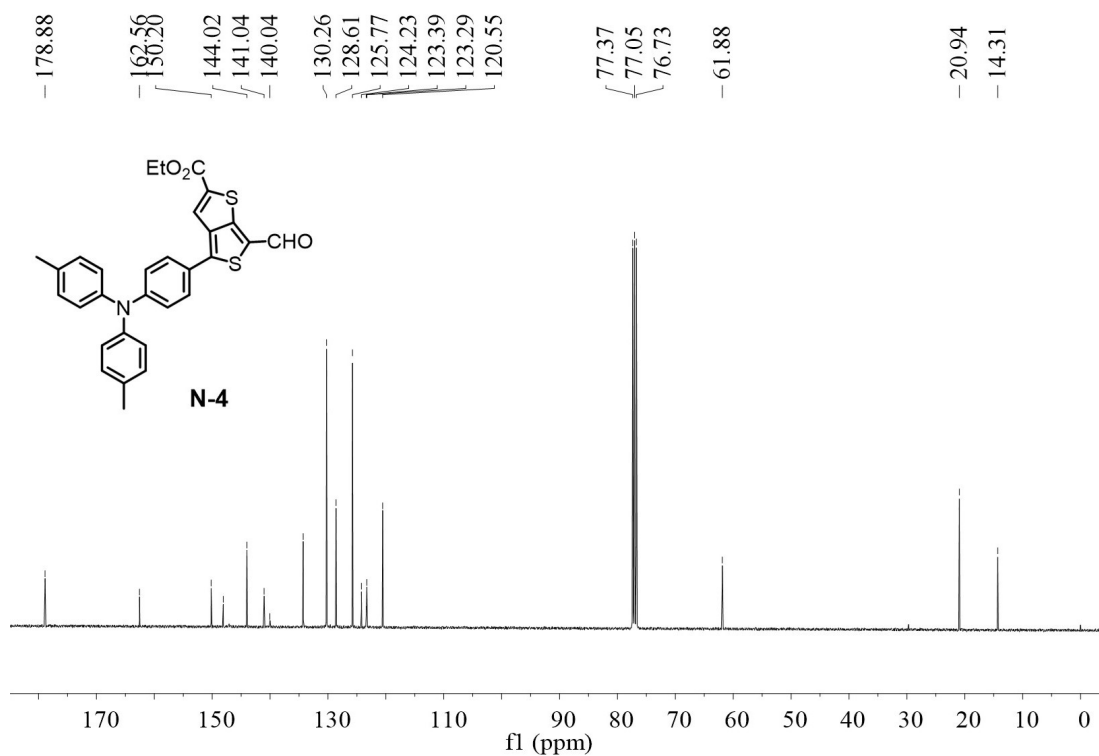*Fig. S6*. ^{1}H NMR spectrum of N-3 in CDCl$_3$.

Fig. S7. ^{13}C NMR spectrum of N-3 in CDCl$_3$.
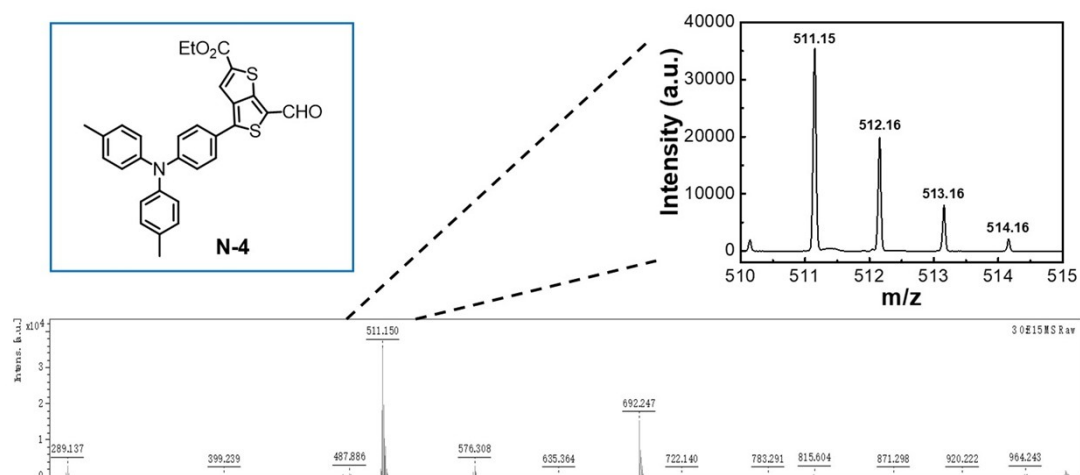
Fig. S8. MALDI-TOF of N-4.
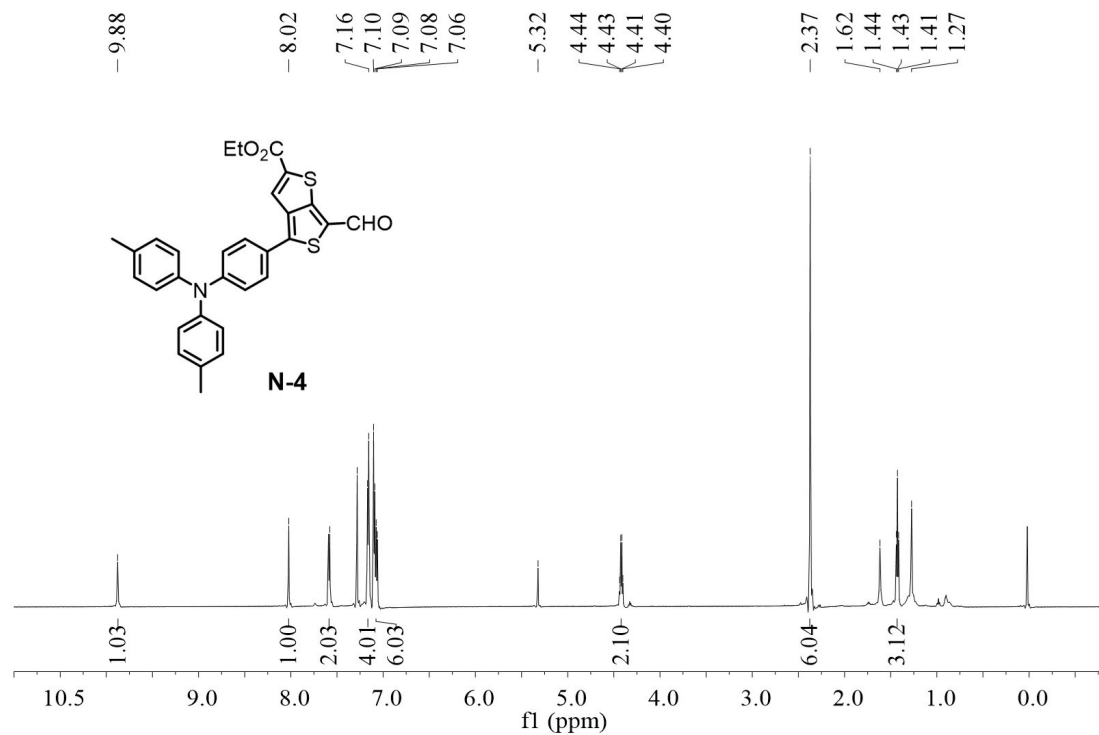
Fig. S9. ^{1}H NMR spectrum of N-4 in CDCl$_3$.
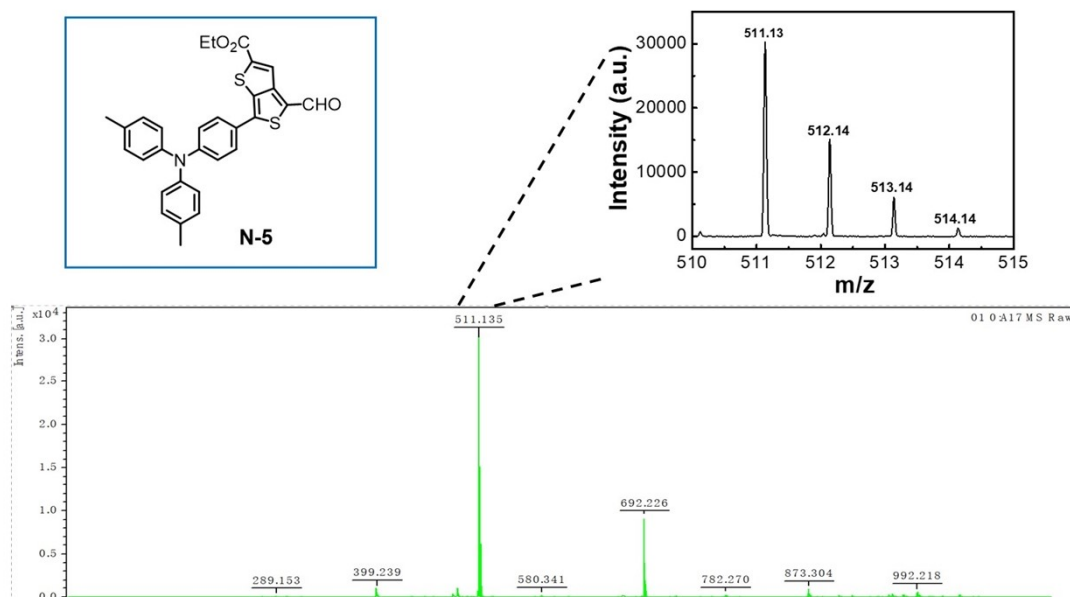

Fig. S10. ^{13}C NMR spectrum of N-4 in CDCl$_3$.
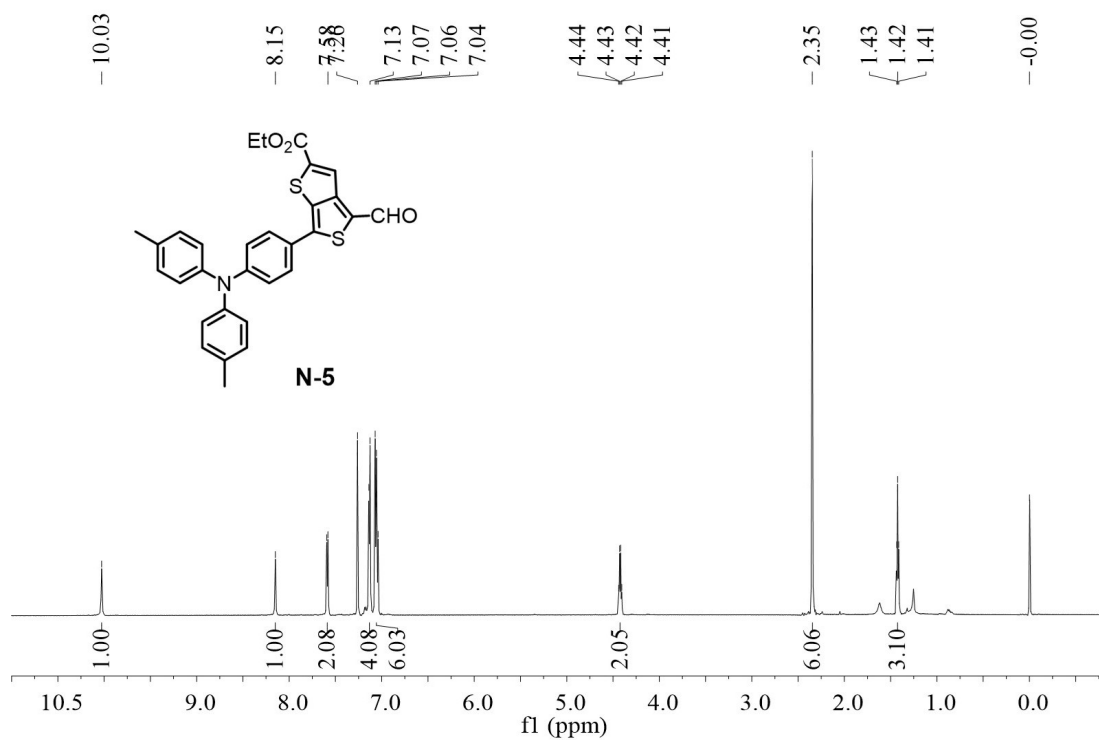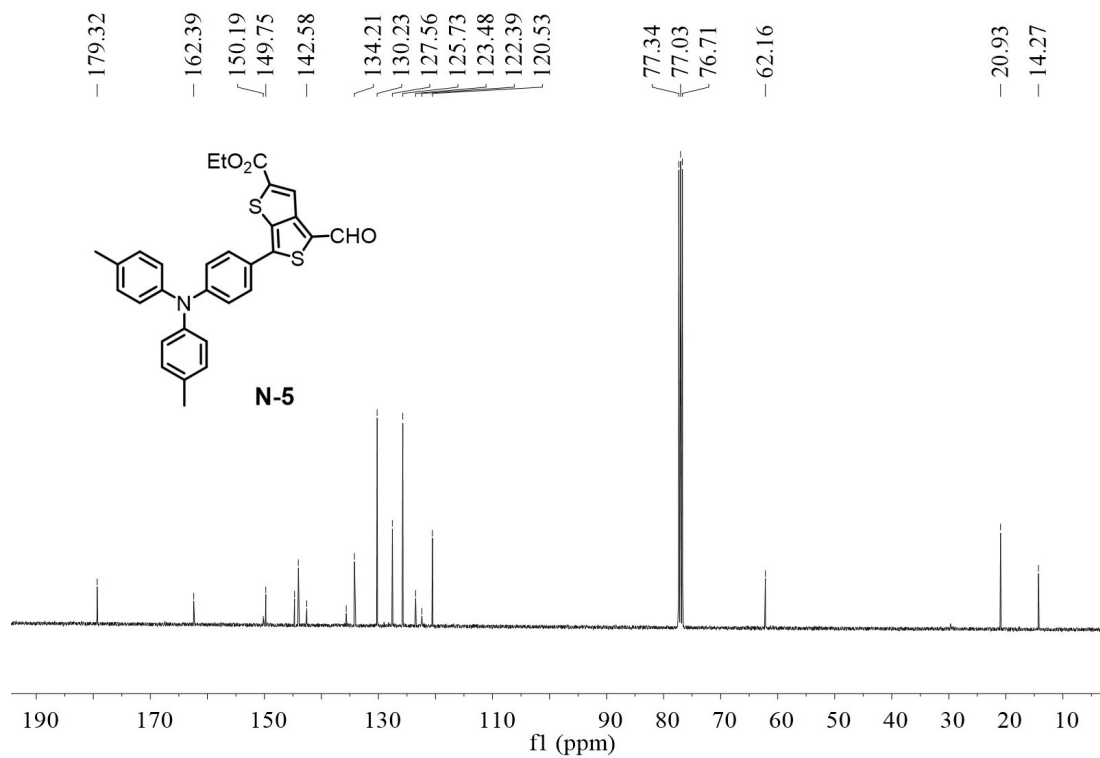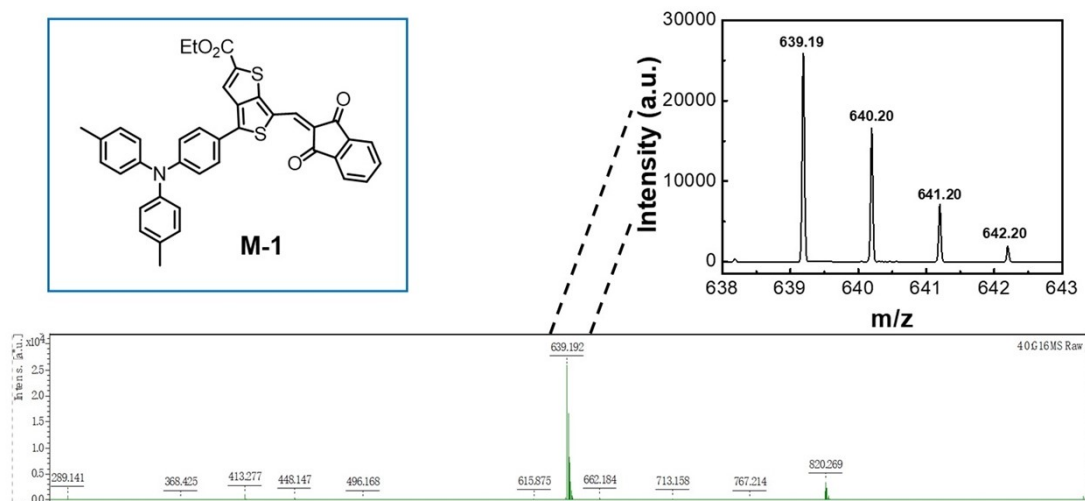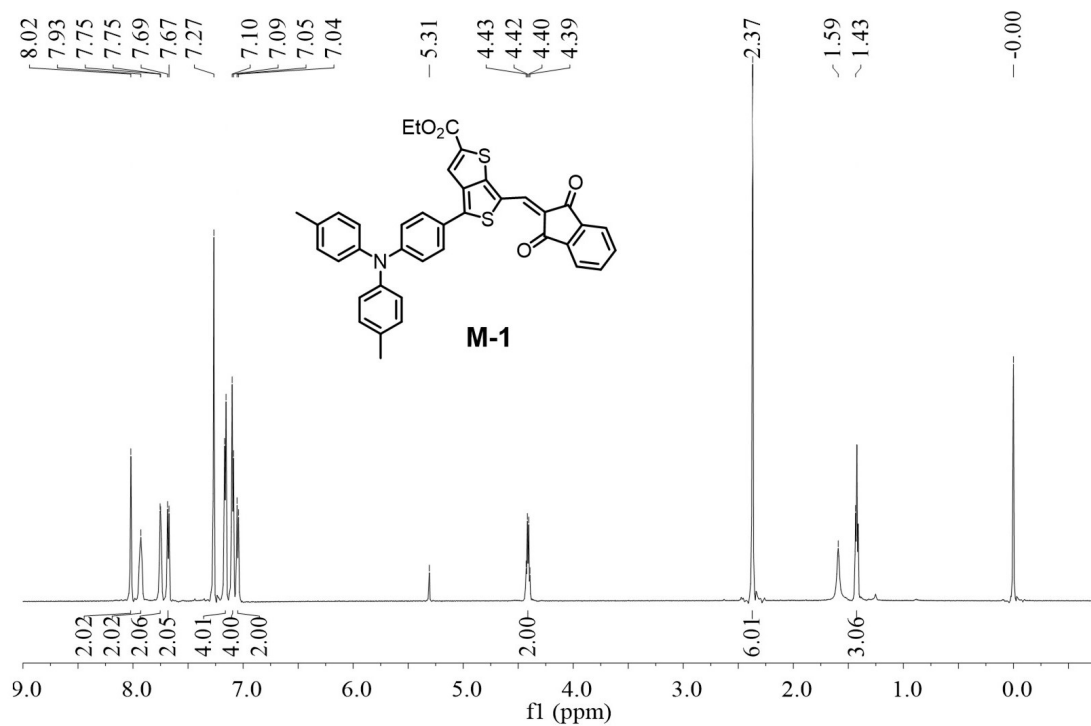
Fig. S11. MALDI-TOF of N-5.

Fig. S12. ^{1}H NMR spectrum of N-5 in CDCl$_3$.

Values above spectrum: 179.32, 162.39, 150.19, 149.75, 142.58, 134.21, 130.23, 127.56, 125.73, 123.48, 122.39, 120.53, 77.34, 77.03, 76.71, 62.16, 20.93, 14.27

N-5

190 170 150 130 110 90 80 70 60 50 40 30 20 10
f1 (ppm)

Fig. S13. ^{13}C NMR spectrum of N-5 in CDCl$_3$.

M-1

639.19
640.20
641.20
642.20

Intensity (a.u.)

638 639 640 641 642 643
m/z

30000
20000
10000
0

639.192

40G16MS Raw

289.141 368.425 413.277 448.147 496.168 615.875 662.184 713.158 767.214 820.269

Fig. S14. MALDI-TOF of M-1.

Fig. S15. ^{1}H NMR spectrum of M-1 in CDCl${}_3$.

Fig. S16. ^{13}C NMR spectrum of M-1 in CDCl${}_3$.

Fig. S17. MALDI-TOF of M-2.

Fig. S18. ^{1}H NMR spectrum of M-2 in CDCl$_3$.
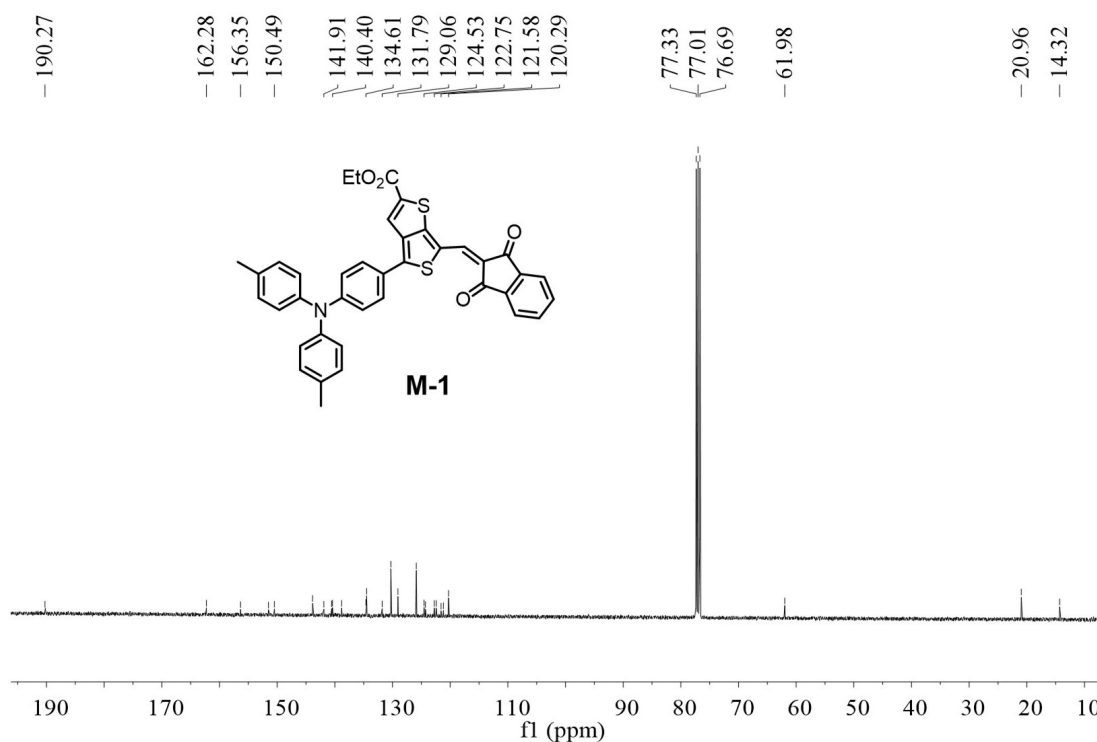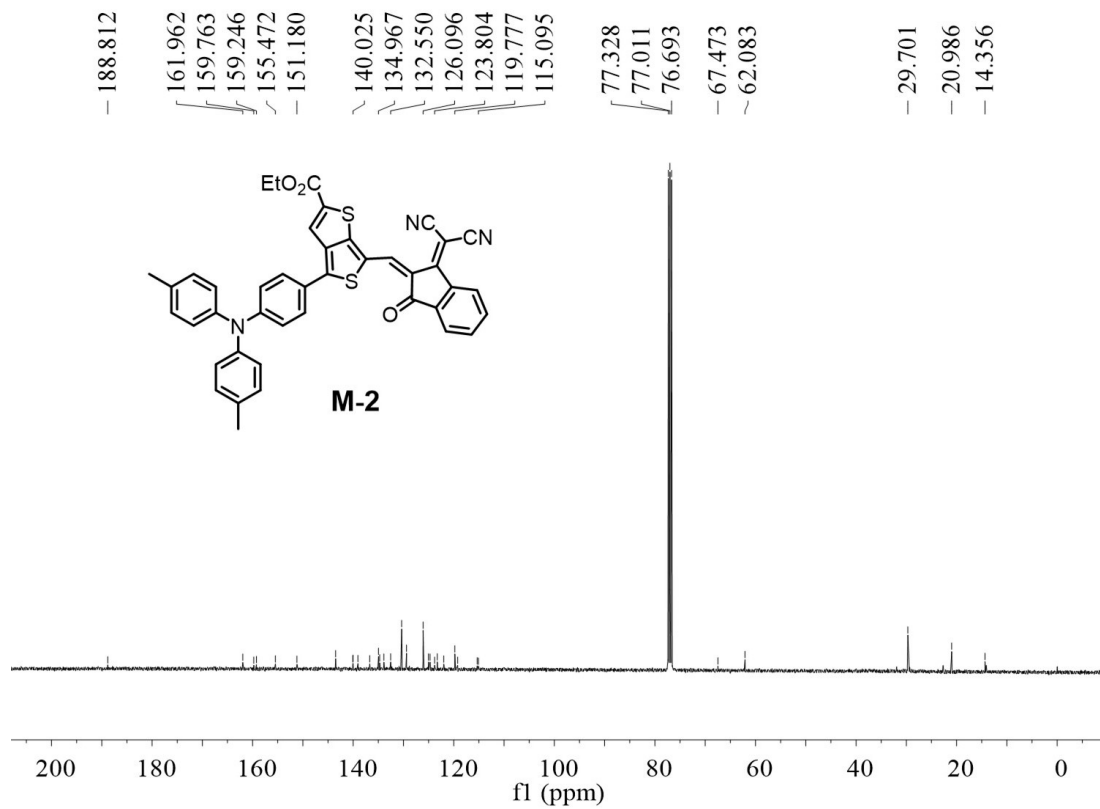
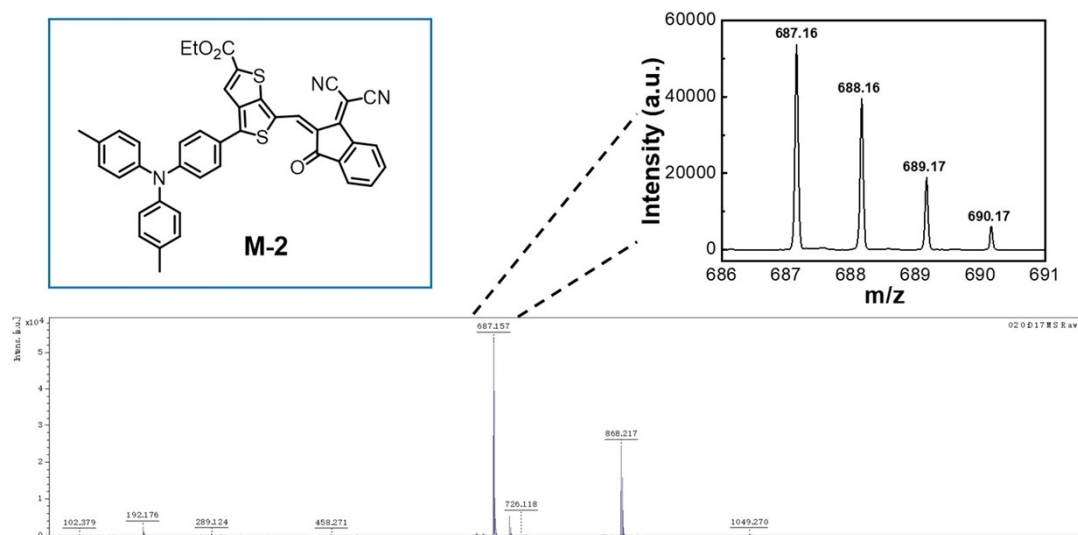*Fig. S19*. ^{13}C NMR spectrum of M-2 in CDCl$_3$.
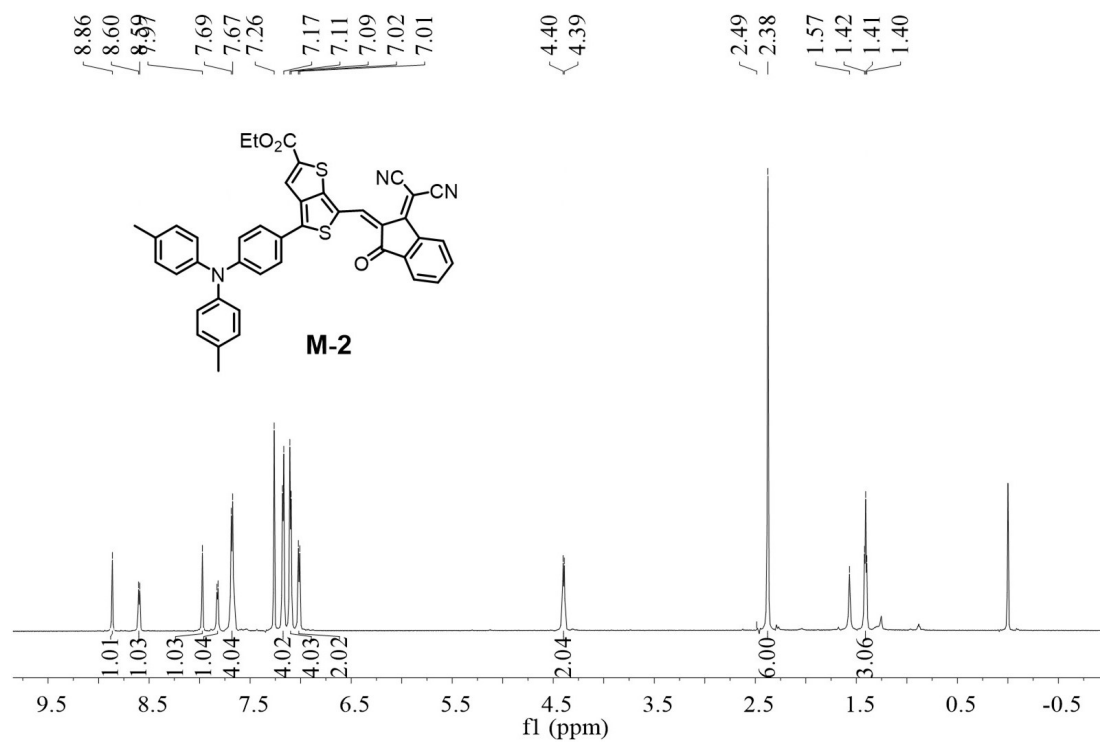

Fig. S20. MALDI-TOF of M-3.

Fig. S21. ¹H NMR spectrum of M-3 in CDCl₃.

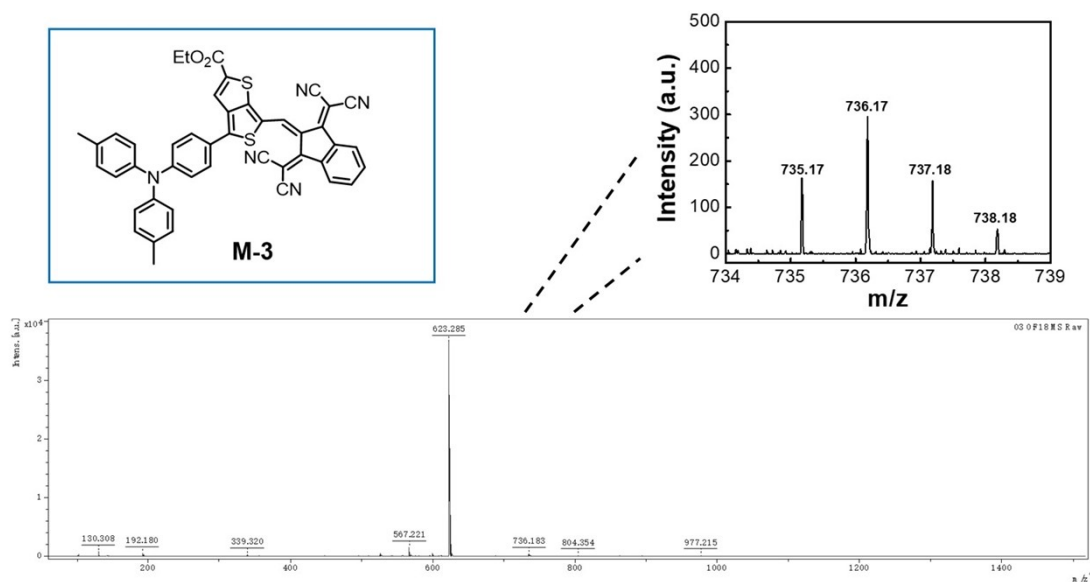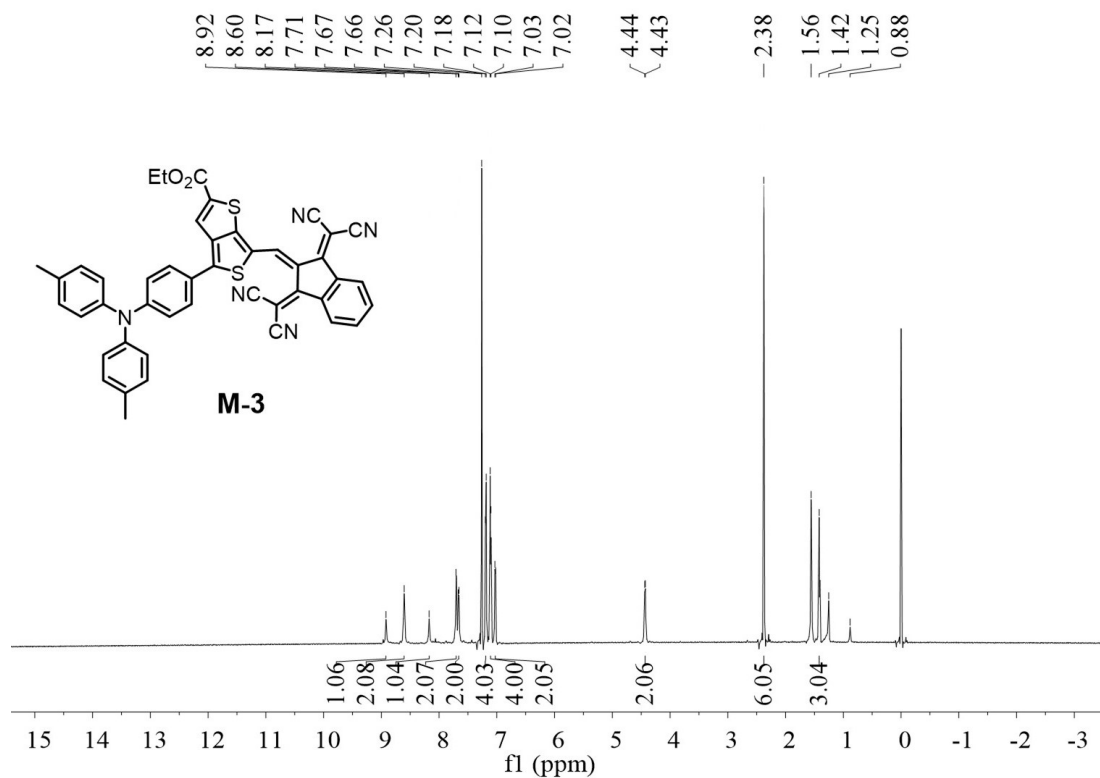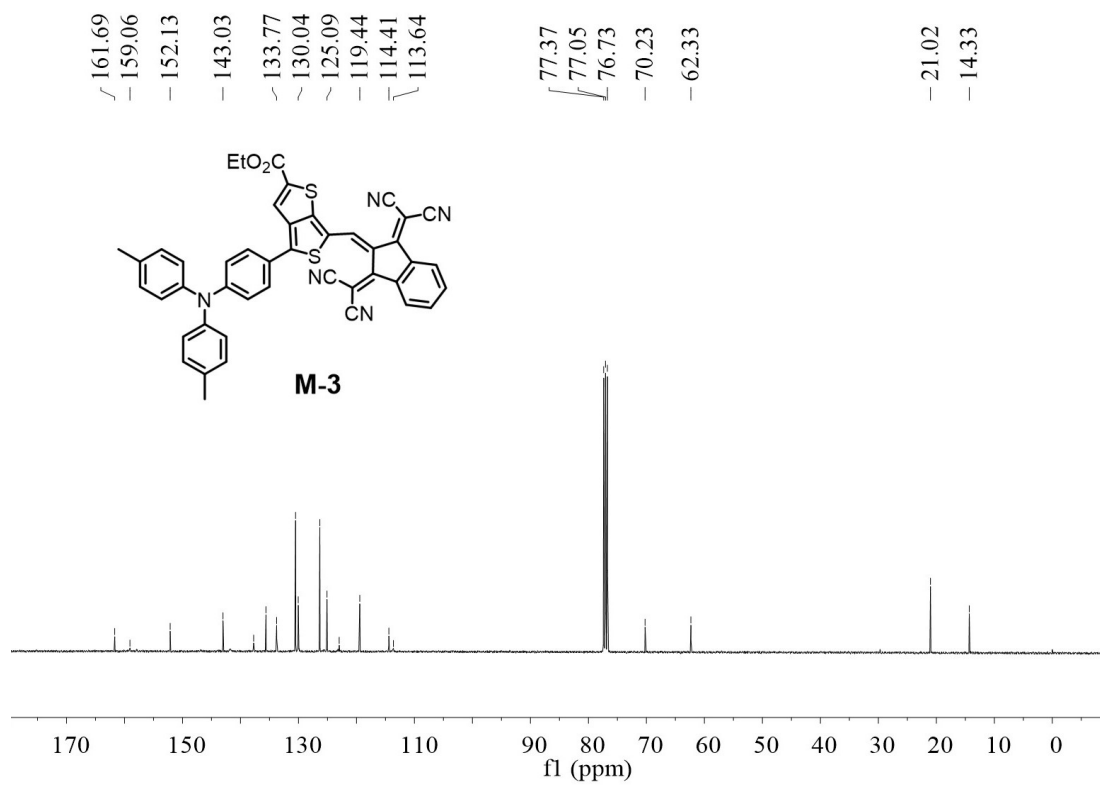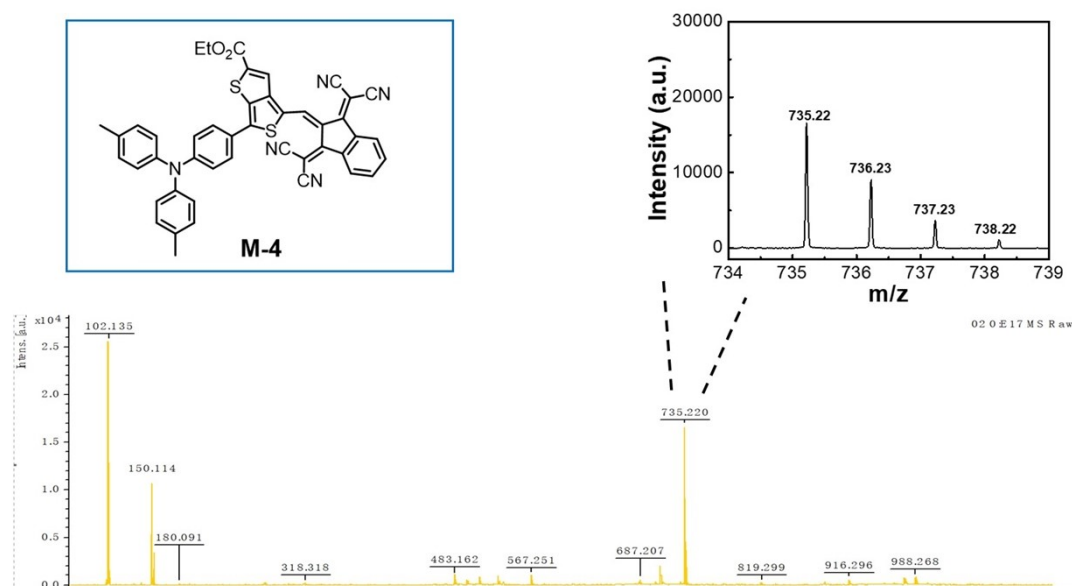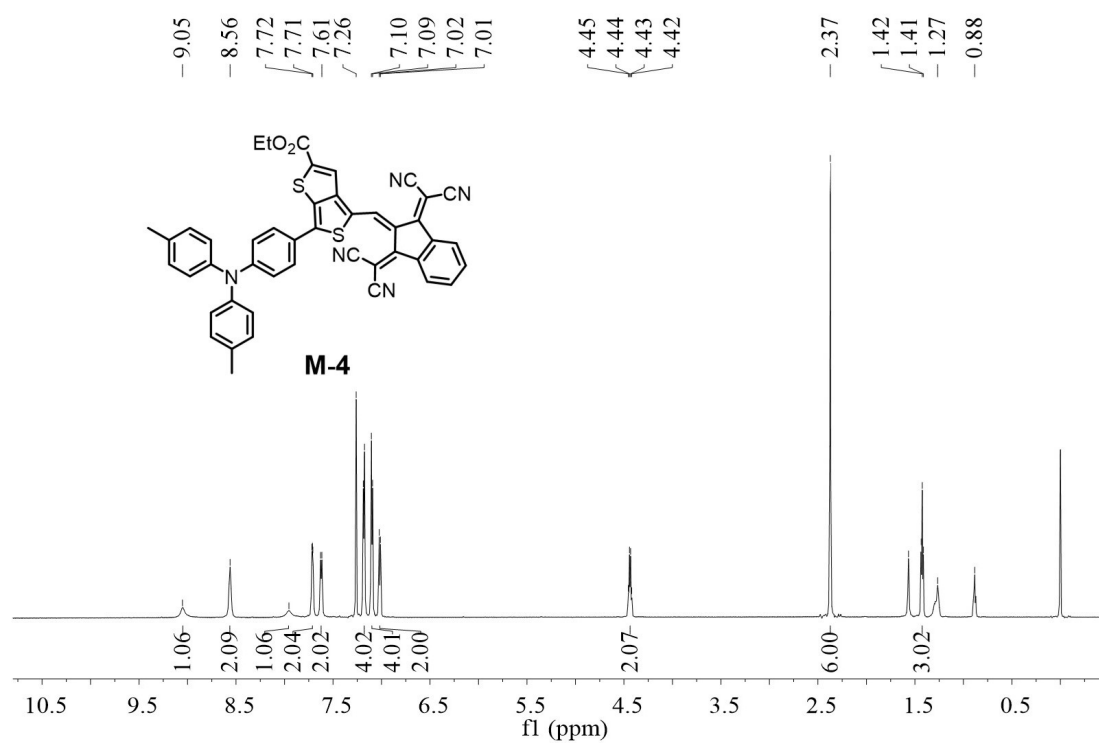**Fig. S22.** ¹³C NMR spectrum of M-3 in CDCl₃.

Fig. S23. MALDI-TOF of M-4.

Fig. S24. ^{1}H NMR spectrum of M-4 in CDCl$_3$.

161.60
160.32
151.79
142.95
130.48
129.24
126.29
125.06
122.11
119.43
114.62
114.36
77.35
77.03
76.72
69.77
62.54
21.02
14.24

EtO$_2$C

NC CN

NC

CN

M-4

170 150 130 110 90 80 70 60 50 40 30 20 10 0
f1 (ppm)
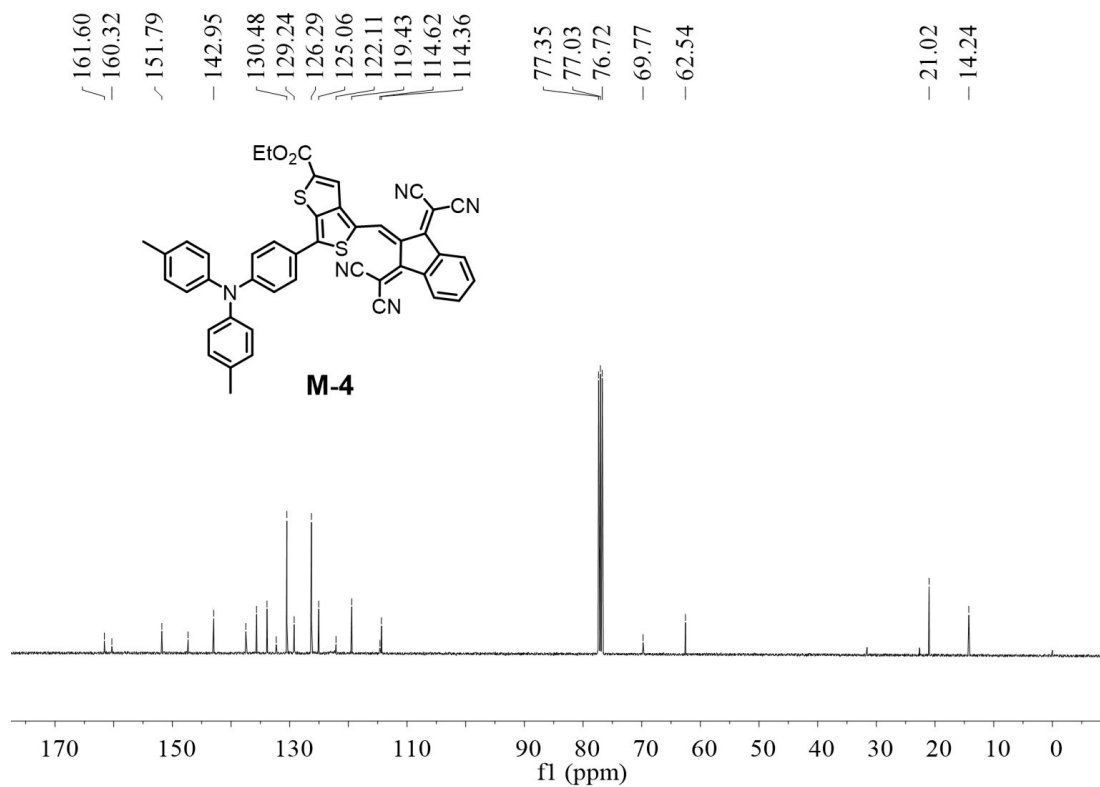
Fig. S25. ^{13}C NMR spectrum of M-4 in CDCl$_3$.
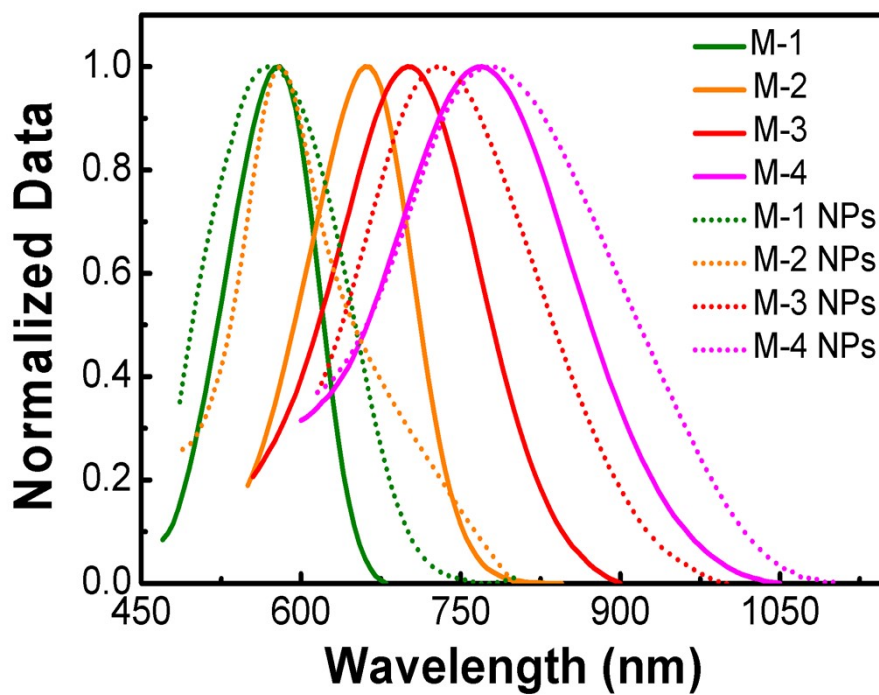
Fig. S26. Normalized absorption spectra of M-1, M-2, M-3 and M-4 in THF and M-1, M-2, M-3 and

M-4 NPs in H$_2$O.
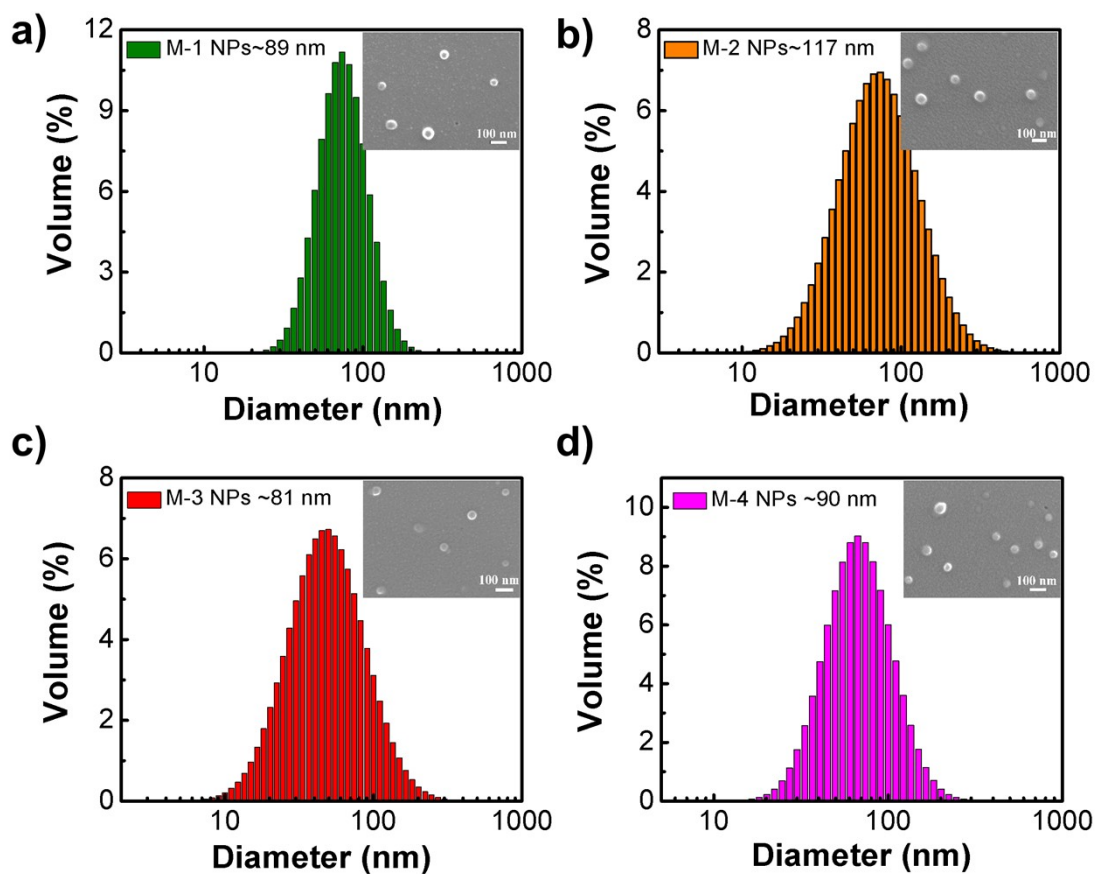
Fig. S27. Size distributions and SEM images of a) M-1 NPs, b) M-2 NPs, c) M-3 NPs, d) M-4 NPs.
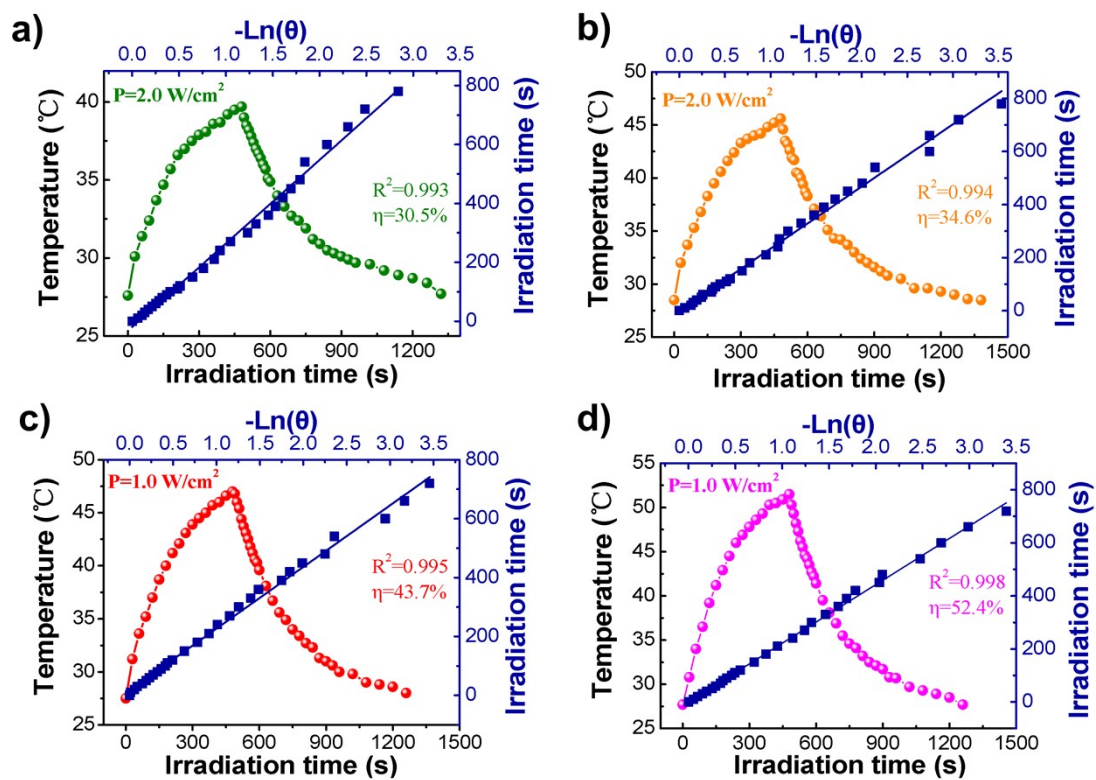
Fig. S28. Photothermal performance of a) M-1 NPs (20 μM, 660 nm, 2 W/cm²), b) M-2 NPs (20 μM, 660 nm, 2 W/cm²), c) M-3 NPs (10 μM, 808 nm, 1 W/cm²), and d) M-4 NPs (10 μM, 808 nm, 1 W/cm²) by cooling to room temperature with linear analysis.

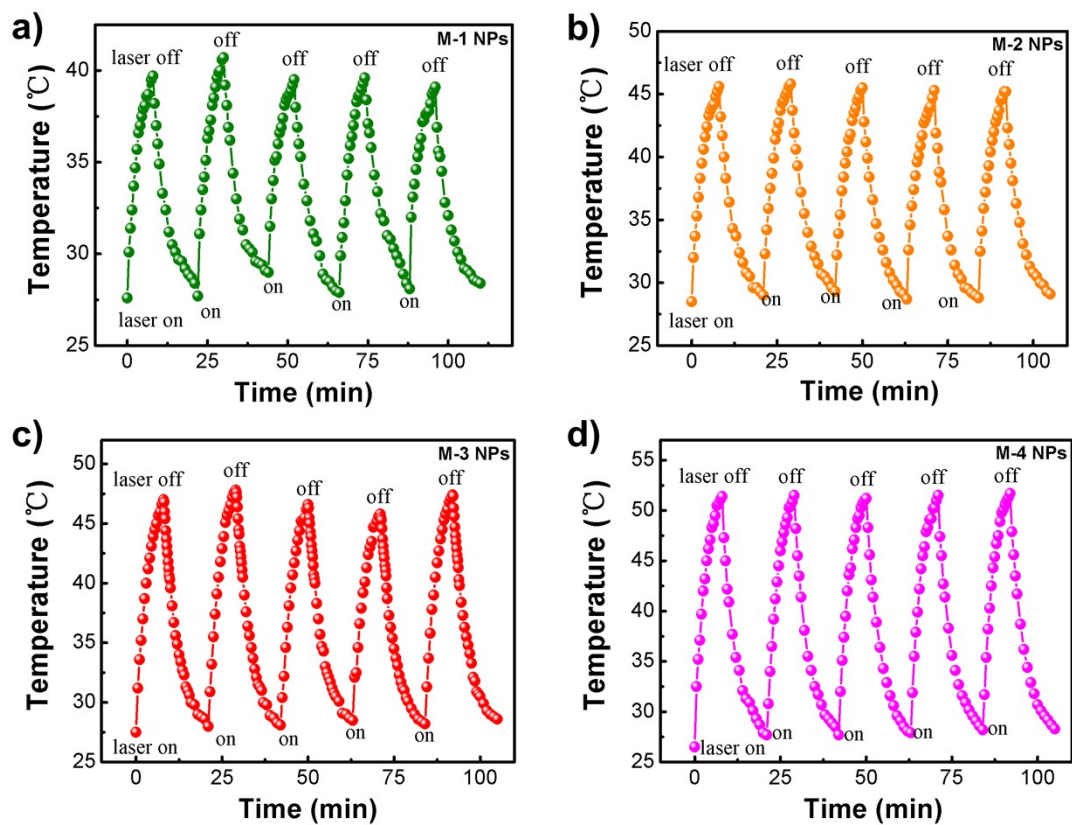***Fig. S29***. Photothermal stability of a) M-1 NPs and b) M-2 NPs upon 660 nm laser irradiation (20 μM, 2 W/cm^2). Photothermal stability of c) M-3 NPs and d) M-4 NPs upon 808 nm laser irradiation (10 μM, 1 W/cm^2).
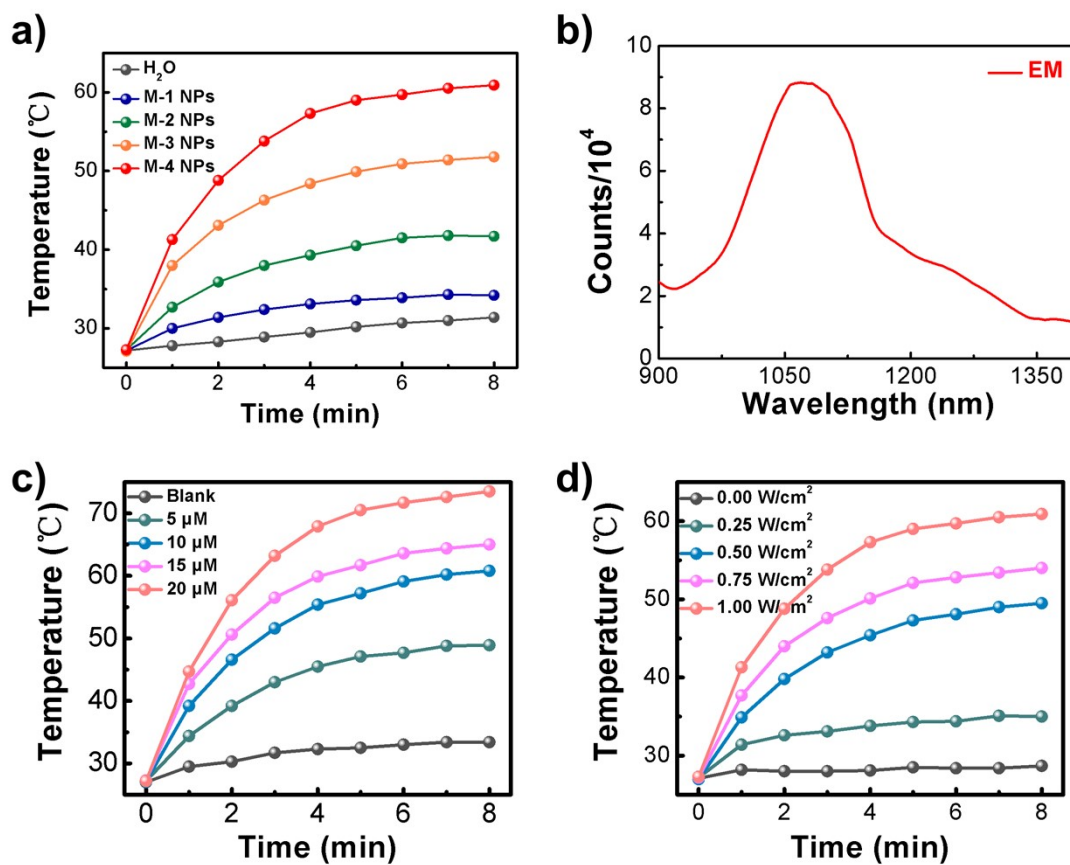
Fig. S30. a) Temperature changes of M-1 NPs, M-2 NPs, M-3 NPs and M-4 NPs (10 μM) in H_2O
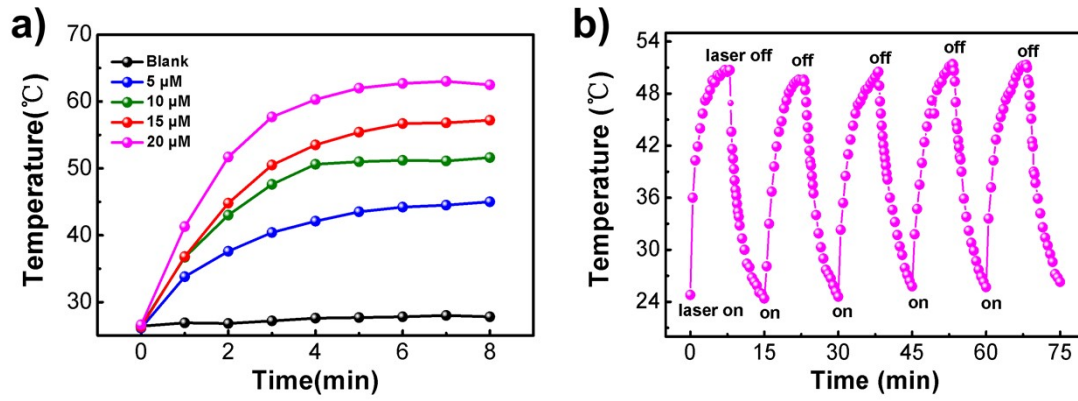
under laser irradiation. b) PL spectrum of M-4 in solid state. c) Photothermal curves of M-4 NPs at

different concentrations (0, 5, 10, 15, 20 μM) under 808 nm (1 W/cm^2) laser irradiation. d)

Photothermal curves of M-4 NPs (10 μM) under 808 nm laser irradiation at different power density

(0.00, 0.25, 0.50, 0.75, and 1.00 W/cm^2).

Fig. S31. a) Photothermal properties of AMDR hydrogels under irradiation of 808 nm laser (1 W/cm^2) containing different concentrations of M-4 NPs (0, 5, 10, 15, 20 µM). b) Photothermal stability of AMDR hydrogel with M-4 NPs concentration of 10 µM under irradiation of 808 nm laser (1 W/cm^2).
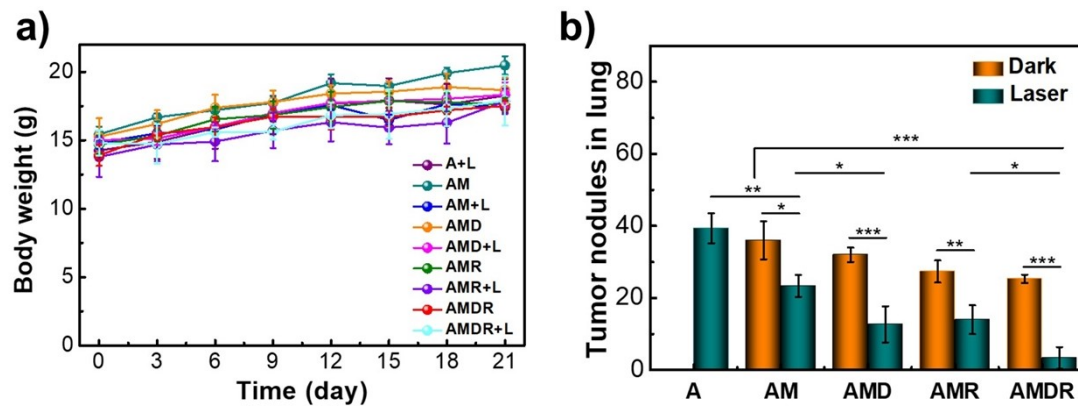
Fig. S32. a) Body weight changes of mice during different treatments. b) Numbers of tumor metastatic nodules in lung of mice (n = 5) after different treatments for 21 days. *p < 0.05, **p < 0.01, and ***p < 0.001.